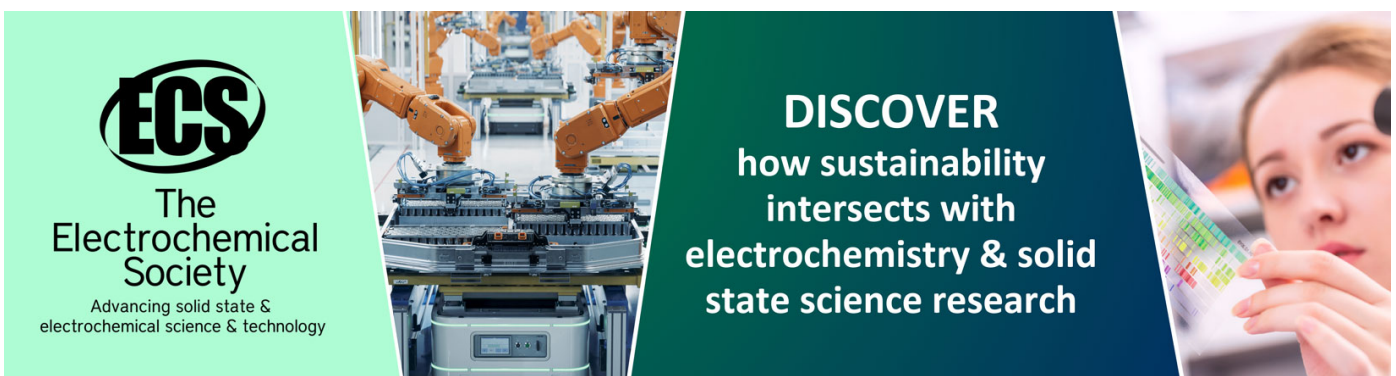**PAPER • OPEN ACCESS**

Effect of friction stir processing on tribological properties of Al-Si alloys

To cite this article: S M Aktarer *et al* 2017 *IOP Conf. Ser.: Mater. Sci. Eng.* **174** 012061

View the article online for updates and enhancements.

Effect of friction stir processing on tribological properties of Al-Si alloys

S M Aktarer[1], D M Sekban[2], H Yanar[3] and G Purçek[3]

[1] Department of Automotive Technology, RecepTayyip Erdogan University, Rize,Turkey
[2] Department of Naval Architecture and Marine Engineering, Karadeniz Technical University, Trabzon,Turkey
[3] Department of Mechanical Engineering, Karadeniz Technical University, Trabzon, Turkey

Email: purcek@ktu.edu.tr

Abstract. As-cast Al-12Si alloy was processed by single-pass friction stir processing (FSP), and its effect on mainly friction and wear properties of processed alloy was studied in detail. The needle-shaped eutectic silicon particles were fragmented by intense plastic deformation and dynamic recrystallization during FSP. The fragmented and homogenously distributed Si particles throughout the improve the mechanical properties and wear behavior of Al-12Si alloy. The wear mechanisms for this improvement were examined and the possible reasons were discussed.

1. Introduction

Al-Si alloys has been extensively used in the automotive, aerospace and military applications duo to their superior wear resistance, low coefficient of thermal expansion, high corrosion resistance, high strength-to-weight ratio and excellent castability [1, 2]. However, they generally have insufficient strength, low fracture toughness and poor ductility which limit their broader applications in the as-cast state [3]. Some traditional processes like alloying, variation in solidification rates, heat treatments and stirring during solidification have been applied to solve or decrease their aforementioned problems [1-4]. Although some improvements in their properties have been achieved with such traditional processes, further improvements are needed in their strength, ductility, impact toughness and wear resistance to be able to enhance their applications. Also, the casting defects like porosity, compositional inhomogeneity, coarse and inhomogeneous Si distribution could not be eliminated completely by traditional processes [3,5,6]. Thus, some novel processes including severe plastic deformation (SPD) have been applied to such kind of alloys so far. Among them, equal-channel angular extrusion/pressing (ECAE/P) [1,2,7], high pressure torsion (HPT) [8,9], accumulative roll-bonding (ARB) [10] and recently friction stir processing (FSP) [3-5,11-25] seem to be the viable methods to improve the mechanical properties of Al-Si alloys.

Considering the surface properties and microstructural modification in the large-scale plate- or sheet-type materials, the FSP can be said the best one among others. FSP is a method of changing the properties of a metal through severe, localized plastic deformation which is produced by forcibly

inserting a non-consumable tool into the work piece, and revolving the tool in a stirring motion as it is pushed laterally through the work piece [5,26]. This process mixes a material without changing the phase and creates a microstructure with fine, equiaxed and uniformly distributed grains and/or particles. After this process, the processed zone is constituted generally by recrystallized fine grains, fragmented primary particles and uniformly distributed second phase particles. FSP method has been applied to Al-Si alloys in the hypoeutectic [18,19,23], near eutectic [13-15] and hypereutectic compositions [3, 20]. These studies have generally focused on the microstructural evolution and mechanical characteristics of plastic deformation during FSP. In addition, the fatigue and crack growth behaviors [6,9,19,26], microstructural modification [5, 22], mechanical properties [11,22,24,26], superplasticity [13] and wear behavior [3,15,17] of Al-Si alloys after FSP have been investigated.

In view of above, there are many reports on Al-Si alloys including different additional alloying elements. However, few of them were on the as-cast binary Al-Si alloys. Also, the effect of FSP on the microstructural evolution including the combination of strength, ductility and also wear properties of the as-cast Al–Si alloys has not been investigated systematically [3]. Furthermore, more studies are needed for getting further improvement in mechanical properties of Al-Si alloys by applying FSP with optimum parameters. Therefore, the main purpose of this study is to modify the surface structure of eutectic as-cast Al-12Si alloy by FSP, and investigate its microstructural, mechanical and tribological properties.

2. Experimental Procedure

Eutectic Al-12wt.%Si alloy was produced by ingot metallurgy with a chemical composition of 12.2%Si, 0.6%Fe, 0.1%Cu, 0.4%Mn, 0.1%Mg, 0.1%Zn, 0.1%Ni, 0.15%Ti, 0.1%Pb, 0.05%Sn and balance Al. The ingots were re-melted in a graphite crucible for getting uniform as-cast microstructure and poured at 650 ^{0}C into a mild steel permanent mold stayed at room temperature. For FSP, the plates having dimensions of 200mm x 40mm x 5mm were produced from the re-casted ingots. Two-pass FSP was performed using a tool steel with a shoulder diameter of 16 mm, a threaded pin diameter of 5 mm and length of 2.5 mm. During the experiments, the tool rotation and traverse speeds were fixed at 1250 rpm and 65 mm.min-1, respectively. The tool was tilted 3°, and downforce of the tool was kept constant at 3kN.

Samples for metallographic investigation were sectioned perpendicular to the process direction from the as-cast ingot by wire-EDM technique (figure 1). After then, they were prepared using standard polishing techniques and then etched in a 10%NaOH solution. The microstructural characteristics of the alloy before and after FSP were investigated using an optical microscope. Tensile properties of the samples were determined using dog-bone shaped specimens with the dimensions of 2 mm x 3 mm x 26 mm using the same wire-EDM technique. The tensile specimens were cross-sectioned parallel to the process direction (figure 1). The tests were performed using an Instron-3382 electro-mechanical load frame at a strain rate of 5.4 x 10-4 s-1. This strain rate was especially chosen to be able to stay into the into the quasi-static deformation range. Hardness specimens were cross-sectioned parallel to the process direction (figure 1) with 2 mm depth. Hardness measurements were performed using a Vickers micro-hardness tester operated at HV0.5. The measurements were carried out on both longitudinal and transverse sections of the FSPed plates.

Dry sliding wear tests of the as-cast and friction stir processed alloy samples were conducted under dry sliding conditions using a pin-on-disc type tribometer (UTS Tribometer T10/20) at room temperature (20°C) and a relative humidity of about 75%. The samples (15 mm x 15 mm x 5 mm) were cut from processed and unprocessed material using the wire-EDM technique. The wear experiments were conducted using a 6 mm diameter Al2O3 ball. In this study, working with a ball shaped counter-face (it is suitable especially for such kind of comparative studies according to ASTM G-99) were preferred. The wear tests were performed for a total sliding distance of 100 m corresponding to a period of 16 min under four different constant loads (2.5N, 5N, 7.5N and 10N) using a sliding speed of 0.1 ms^{-1}. Wear rate was defined by measuring mass loss of alloy at the end of every sliding distance with using a microbalance with an accuracy of ±0.1 mg. Prior to the wear tests,

all sample surfaces were ground using emery paper with a grit size of 1200, which yielded an approx. 0.1 µm roughness (Ra) on the sample surfaces for all conditions before the wear tests.
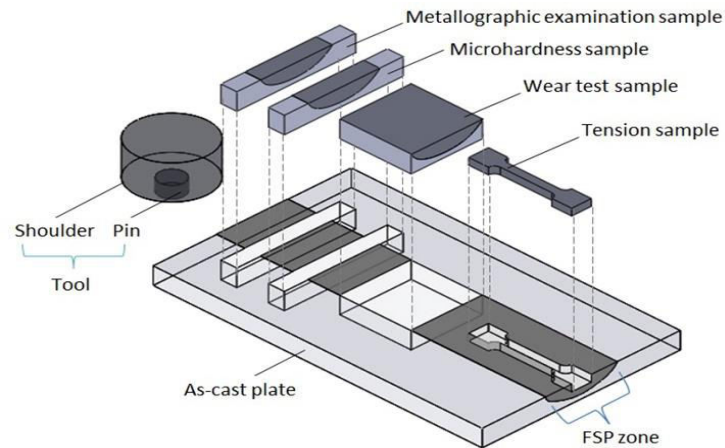

Figure 1. Schematic illustrations of the FSPed plate and the sample geometries machined from that plate.

3. Results and Discussion

3.1. Microstructure

Figure 2 (a) shows optical micrograph of as-cast Al-12Si alloy. It consists of eutectic Si particles (dark), α-Al phase (white), and few coarse primary silicon particles (dark). Eutectic Si particles exhibited a fibrous morphology and it is in the form of acicular or needle-shaped plates dispersed throughout the α-Al matrix. The presence of large primary Si particles was also observed in the microstructure due to the non-equilibrium cooling and slight variations in the eutectic composition. This is a typical structure of as-cast eutectic Al-Si alloy [1,4,5]. The effect of FSP on the microstructure of as-cast Al-12Si alloy is shown in Figure 2(b). The effect of FSP on the shape, size and size distribution of the eutectic Si particles dispersed in the matrixes are more pronounced as compared to other constituents. The Si particles after two-pass FSP are nearly equiaxed in shape and uniform in size and distribution than the particles in the as-cast condition. Finally, the microstructure of the FSPed alloy in the nugget zone (NZ) consists of fine eutectic silicon particles with uniformly distribution throughout the NZ [23]. The fracture in coarse primary Si particle seems to be inconsiderable. The structure in the Figure 2 (b) appears to be partially recrystallized where some fine Si particles started to form within the elongated Si particles. Such structural formation has also been reported in many Al alloys [3,23].
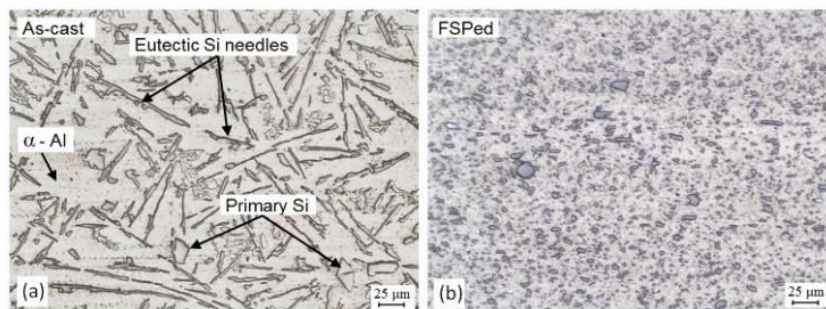

Figure 2. Microstructures: (a) Microstructure of as-cast Al-12Si alloy and (b) microstructure of friction stir processed Al-12Si alloy.

3.2. Mechanical Properties

The engineering stress-engineering strain curves of the Al-12Si alloy before and after FSP are shown in figure 3, and the values of strength and ductility that obtained from these curves are given in table 1. As-cast alloy exhibited a typical stress–strain curve for a brittle material with poor uniform and total elongations. After FSP, this curve changed to a typical ductile material's curve with a large strain hardening region. Therefore, the strength and ductility of the alloy increased simultaneously by the effect of FSP. The alloy sample showed an increase in the ultimate tensile strength (σ_{UTS}) of about 48%, from 148 MPa for the as-cast sample to about 220 MPa for the FSPed sample. Similarly, the yield strength increased about 32% after FSP, from 100 MPa to 132 MPa. In addition, while the σ_{UTS}/σ_Y ratio is 1.48 in the as-cast alloy, this ratio increased after FSP to about 1.66, which meant that the strain hardening region increased with FSP. The ductility of the alloy also increased substantially after FSP. The FSPed sample exhibited considerably higher elongation to fracture (ε_f) of about 23% in comparison with no processed sample having only 3.7%, which was almost 6.2 times higher than that of the as-cast sample. More importantly, uniform elongation (ε_u) increased considerably after FSP in contrast to other UFG materials. It increased from 2.9% in the as-cast state to about 14% after FSP. The simultaneous increase in strength and ductility of the alloy after FSP was attributed to the changes in microstructure during FSP. It is well known that the mechanical properties of Al-Si alloys strongly depend on the shape, size and distribution of silicon particles, porosities and also the size of α-Al matrix phase [1, 5, 15, 24]. Needle shaped silicon particles dispersed in the matrix acts as an internal stress raiser, which raises the cracking tendency of the alloy. Therefore, the as-cast alloy exhibited low strength and very poor ductility at room temperature. During FSP, the as-cast morphology is completely broken up especially in the NZ (figure 2). The extensive friction stir effect during processing results in significant changes in Si particle morphology by breaking them into smaller particles. Finally, disintegration/fragmentation and better distribution of eutectic silicon particles form in the matrix after FSP, which leads to extraordinary improvement in strength and ductility of the alloy.

The as-cast Al-12Si alloy exhibited hardness values varying between 52Hv0.5 and 66Hv0.5 which indicates highly scattered hardness distribution inside the as-cast structure. The average value is 58 Hv0.5 for the as-cast structure. This is a normal as considering the inhomogeneous distribution of coarse eutectic Si particles as well as casting defects inside the as-cast microstructure (figure 2(a)). Because, there is a more chance that the hardness indenter may press on the places with or without Si particles in coarse-grained as-cast structure. Two-pass FSP increased the hardness of the alloy inside the NZ. The sample shows an increase in the hardness of about 15%, from 58 Hv0.5 for the un-processed as-cast zone to about 67 Hv0.5 for the NZ. This is primarily due to the increase in dispersion hardening effect of refined and more uniformly distributed eutectic silicon particles in the α-Al matrix by the effect of FSP [11,15]. Also, the α-Al matrix phase refines due to the dynamic recrystallization during FSP, which provides additional improvement in hardness of this zone [25, 26]. The NZ zone, on the other hand, have more uniform hardness distribution with fewer scatter as reported in some previous studies on Al-Si alloys [3, 5,11,15,18, 20, 24]. The hardness profile is relatively smooth (ranges from 63 HV to 67 HV), and less scatters form inside the NZ. This can be attributed to the fine and more uniformly distributed eutectic Si particles in the NZ of FSPed sample.

Table 1. Tensile properties and hardness of the as-cast and FSPed Al–12Si alloy (σUTS: Ultimate Tensile Strength, σY: Yield Strength, εf: Elongation to Failure, εu: Uniform Elongation, HV0.5: Hardness Vickers).

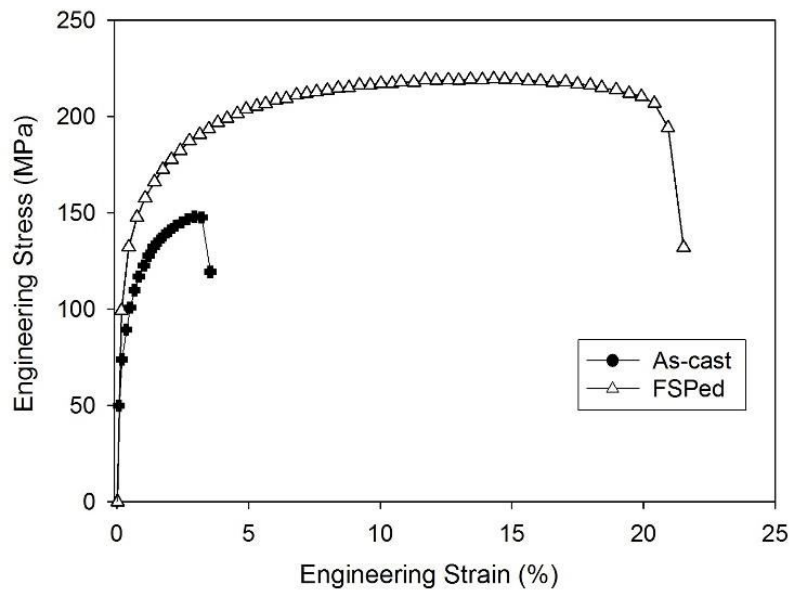|	σ_{UTS} (MPa)	σ_Y MPa)	ε_f (%)	ε_u (%)	σ_{UTS}/σ_Y	HV0.5
As cast	148 ± 6	100 ± 5	3.7 ± 0.3	2.9 ± 0.5	1.48	58
FSPed	220 ± 3	132 ± 4	23.0 ± 1.1	14.0 ± 0.6	1.66	67

Figure 3. Engineering stress–strain curves of the as-cast and
FSPed Al–12Si alloy.

3.3. Friction and Wear Behavior

Figure 4 shows the coefficient of friction versus sliding distance curves for the alloy before and after FSP. The figure shows a high initial value, about 1.09 in friction coefficient during the initial transient-state sliding period with steady-state levels reached after about 10 m for both conditions, which demonstrates that no considerable changes occur after microstructural alteration by FSP. The average coefficient of friction in the steady-state condition for both conditions is about 0.5.
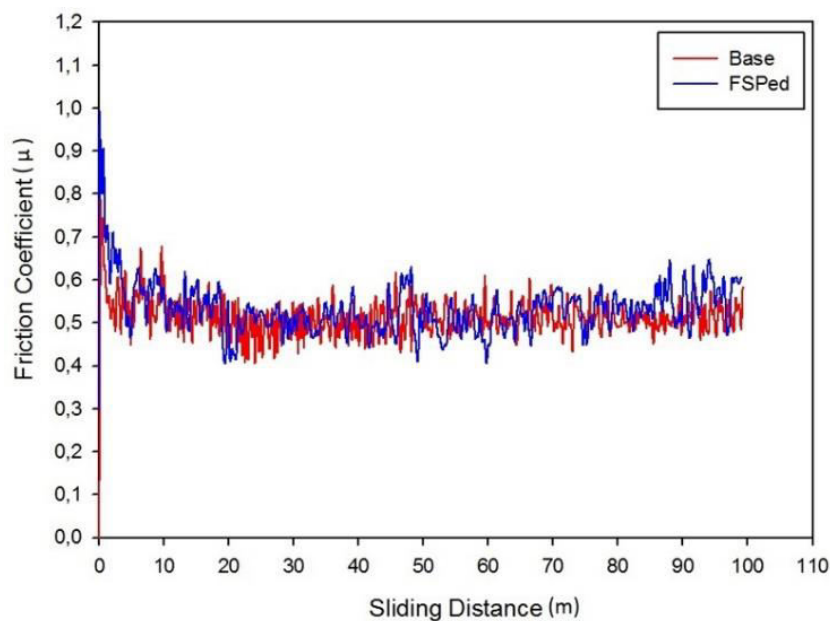

Figure 4. The coefficient of friction vs. sliding distance curves
for Al-12Si alloy before and after FSP.

Figure 5 shows a typical relationship between the weight loss and applied normal load of the as-cast and FSPed Al–12Si alloy. It reveals that the weight loss increases almost linearly with increasing applied load for the Al–12Si alloy in both conditions. The results show that the FSPed samples exhibited significantly lower weight loss for all normal loads compared to the as-cast Al–12Si alloy. But, the difference is more distinct at higher loads. The comparison of the wear behavior of the as-cast and FSPed alloy show that the FSP increased the wear resistance of the alloy considerably by decreasing the weight loss due to the increase in strength and hardness after FSPed for especially high applied load. These results are also confirmed by the 2D and 3D profilometric maps. The effect of applied load on the wear depth and 3D profilometric view of wear tracts of as-cast Al-12Si and FSPed Al-12Si are shown in figure 6. It is clearly seen that both diagrams demonstrate almost the same variation in each case. The wear depth increases with increasing applied load for all conditions, and the increment is more pronounced at higher loads. It is observed that the groove shapes of the base sample and FSPed sample are more-or-less different under different loads, and grove shapes of the samples widens with increasing applied load. The base sample has deeper grooves and wider ridges, which causes more weight/volume loss than FSPed sample under all loads. Also, the 2D profiles of FSPed are smoother than those of base alloy (figure 6). As shown, the base sample has about 70 μm of wear depth while the FSPed sample has about 50 μm of wear depth for 10N applied load.
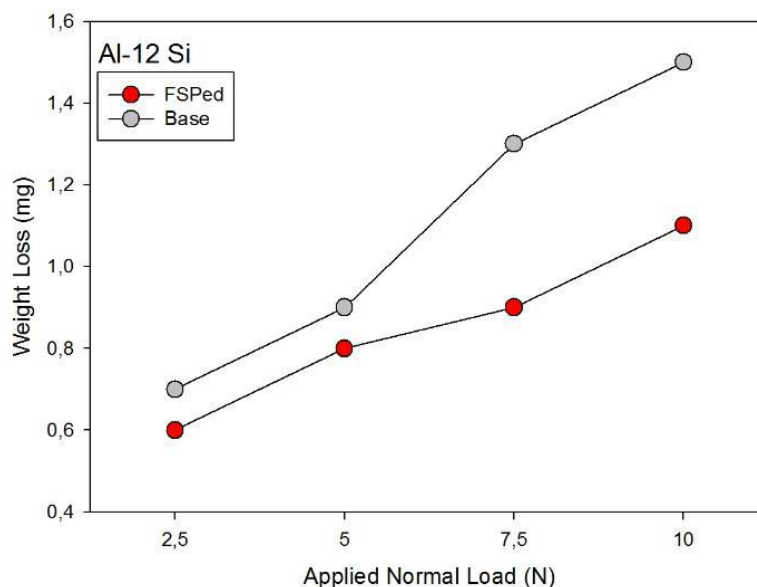

Figure 5. The change in weight loss as a function of applied
load for as-cast and FSPed Al–12Si alloy.

The advancement of the wear resistance after FSP might be connected to the radical microstructural alterations. It is well known that the mechanical properties and wear resistance of Al-Si alloys strongly depend on the shape, size and distribution of silicon particles, porosities and also the size of α-Al matrix phase [1, 3-5, 24]. Needle shaped silicon particles dispersed in the matrix acts as an internal stress raiser, which raises the cracking tendency of the alloy. High stress concentrations along the Si/matrix interfaces, which are responsible for the nucleation and propagation of cracks, may be caused by Si particles with high aspect ratio. When the cracks take place, they may lead to the fragmentation of the large Si particles into smaller and homogenous ones. After a wearing process, those particles may be disengaged from the surface and work as an additional abrasive, thus increase the wear rates [17]. As a result of the Al soft matrix's direct relation to the counterface, the alloy's ability to support the load is reduced by the void left by the disengaged Si particles. The extensive

friction stir effect during FSP results in significant changes in Si particle morphology by breaking them into smaller particles as shown in figure 2. Finally, disintegration/fragmentation and better distribution of eutectic silicon particles form in the matrix after FSP, which leads to improvement in wear resistance of the alloy. The elimination of the porosity, as well as the Si particles refining, contributes notably to the improvement of the wear resistance of Al-12Si alloy. In addition, the fact that stress concentrations may occur around the pores results in an increase in the wear resistance. Also, the hardness of the alloy increases by the effect of FSP, and this bring about a further improvement in wear resistance of FSPed alloy [1,3,4,22]
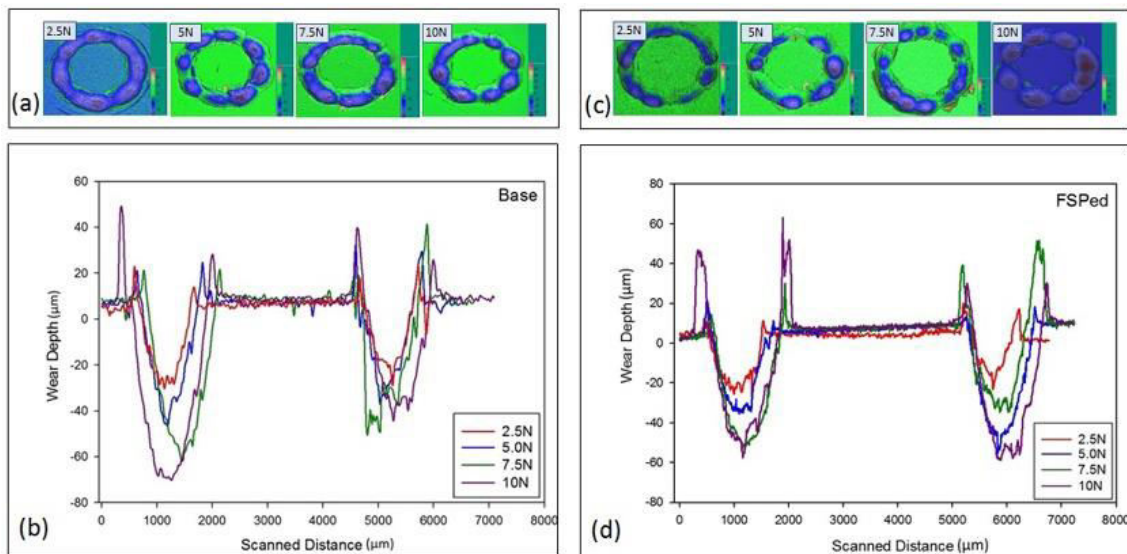

Figure 6. 3D profilometric view of wear tracts of Al-12Si alloy under different loads and 2D view of worn tracts took place under different loads: (a)-(b) As-cast Al-12Si alloy before FSP and (c)-(d) FSPed alloy.

4. Conclusions

Friction stir process technique was applied to the as-cast eutectic Al–12Si alloy to improve their friction and wear properties. The main findings and conclusions of this study can be summarized as follows:

1. Both strength and ductility of the as-cast eutectic Al–12Si alloy increased considerably as well as hardness after a two-pass process. This simultaneous increase in strength and ductility was mainly attributed to the grain refinement and morphological changes in eutectic coarse acicular Si particles as well as coarse primary Si particles. The alloy after FSP exhibited 220 MPa tensile strength and 132 MPa yield strength, which were about 48% and 32% higher than those of the as-cast alloy, respectively.

2. After FSP, there is no significant change in the average coefficient of friction. The FSPed samples and as-cast samples exhibited average coefficient of friction of about 0.5.

3. The weight loss (also volume loss) increased almost linearly with increasing applied load for the as-cast and FSPed Al-12Si alloy. The FSPed samples exhibited significantly lower weight loss especially under high loads compared to the as-cast Al–12Si alloy. The FSPed sample exhibited better wear resistance than the as-cast Al-12Si alloy for especially high applied loads.

4. It can be concluded that the use of microstructural modification by FSP is a simple and effective procedure for providing remarkable improvement in strength, ductility, hardness and wear resistance of as-cast Al-12Si alloys.

References
[1]   Purcek G, Saray O and Kul O 2010 *Met. Mater. Int.* **16** 145-154
[2]   Kucukomeroglu T 2010 *Mater. Desıgn* **31** 782-789
[3]   Mahmoud T S 2013 *Surf. Coat. Tech.* **228** 209-220
[4]   Aktarer S M, Sekban D M, Saray O, Kucukomeroglu T, Ma Z Y and G Purcek 2015 *Mat. Sci. Eng. A-Struct.* **636** 311-319
[5]   Ma Z Y, Sharma S R and Mishra R S 2006 *Metall. Mater. Trans. A* **37a** 3323-3336
[6]   Mishra R S and Ma Z Y 2005 *Mat. Sci. Eng. R* **50** 1-78
[7]   Zhang Z G, Hosoda S, Kim I S and Watanabe Y 2006 *Mat. Sci. Eng. A-Struct.* **425** 55-63
[8]   Gode C, Yilmazer H, Ozdemir I and Todaka Y 2014 *Mat. Sci. Eng. A-Struct.* **618** 377-384
[9]   Abd El Aal M I and Kim H S 2014 *Mater. Desıgn* **53** 373-382
[10]   Kitazono K, Nishizawa S, Sato E and Motegi T 2004 *Mater. Trans.* **45** 2389-2394
[11]   Choi D H, Kim Y H , Ahn B W, Kim Y I and Jung S B 2013 *T. Nonferr. Metal. Soc.* **23** 335-340
[12]   Yang C W, Chang Y H, Lui T S and Chen L H 2012 *Mater. Desıgn* **40** 163-170
[13]   Tutunchilar S, Besharati M K, Haghpanahi M and Asadi P 2012 *Mat. Sci. Eng. A-Struct.* **534** 557-567
[14]   Tsai F Y and Kao P W 2012 *Mater. Lett.* **80** 40-42
[15]   Mahmoud T S and Mohamed S S 2012 *Mat. Sci. Eng. A-Struct.* **558** 502-509
[16]   El-Rayes M M and El-Danaf E A 2012 *J. Mater. Process. Tech.* **212** 1157-1168
[17]   Alidokht S A, Abdollah-zadeh A, Soleymani S, Saeid T and Assadi H 2012 *Mater. Charact.* **63** 90-97
[18]   Karthikeyan L, Senthilkumar V S and Padmanabhan K A 2010 *Mater. Desıgn* **31** 761-771
[19]   Jana S, Mishra R S, Baumann J B and Grant G 2010 *Acta Mater.* **58** 989-1003
[20]   Rao A. G, Rao B R K, Deshmukh V P, Shah A K and Kashyap B P 2009 *Mater. Lett.* **63** 2628-2630
[21]   Jana S, Mishra R S, Baumann J B and Grant G 2009 *Scripta Mater.* **61** 992-995
[22]   Ma Z Y, Sharma S R and Mishra R S 2006 *Scripta Mater.* **54** 1623-1626
[23]   Ma Z. Y, Sharma S R and Mishra R S 2006 *Mat. Sci. Eng. A-Struct.* **433** 269-278
[24]   Santella M L, Engstrom T, Storjohann D and Pan T Y 2005 *Scripta Mater.* **53** 201-206
[25]   Sharma S 2004 *Scripta Mater.* **51** 237-241
[26]   Ma Z Y, Pilchak A L, Juhas M C and Williams J C 2008 *Scripta Mater.* **58** 361-366